

1.4 HEAT TRANSFER

1.4.1 Introduction

Heat transfer is *thermal energy* in transit due to a spatial temperature difference. The second law of thermodynamics tells us that heat is naturally transferred from a high-temperature body to a low-temperature body. Heat transfer has three modes or mechanisms: conduction, convection, and radiation.

Thermal energy involves motions such as the rotation, translation, and vibration of molecules. *Temperature* measures the average kinetic energy of molecules. Molecules in a warmer object have greater kinetic energy than molecules in a cooler object. When a hot object comes in contact with a cold one, the molecules in the hot object transfer some of their kinetic energy during collisions with molecules of the cold object. This transfer of kinetic energy of molecules is the mechanism of conduction and convection heat transfer. *Conduction* usually takes place in a solid.

For example, when we touch a metal spoon in a hot coffee, we feel the hotness. This is due to the conduction in the spoon. *Convection* occurs on the surface of an object with fluid in motion. As another example, think of bare skin, which usually experiences a heat loss to the ambient air by convection heat transfer.

Suppose that the surface temperature of our skin is greater than that of the ambient air. Then air adjacent to the skin gets warm, becoming lighter in density and rising to induce a flow near the skin. This is the mechanism of *free convection*. If our skin is exposed to wind, the mechanism of the heat transfer is called *forced convection*. *Radiation*, or *thermal radiation*, is somewhat different from conduction and convection. Radiation is energy emitted by matter that is at a nonzero temperature. It is *electromagnetic waves* (or *photons*) effectively propagating even in a vacuum. Radiation is generated when the movement of charged particles (molecules and atoms can be easily charged or ionized when they lose electrons) is converted to electromagnetic waves. For example, why do we feel the coldness of outside in winter when we are in a room where the air temperature remains constant through the year? Because the wall's temperature is lower in winter due to conduction. Our body interacts not only by convection with the air but also by the radiation exchange with the walls. Therefore, we have more heat loss in winter than in summer and feel colder. Note that heat transfer always has a direction and a magnitude like a vector, which is very important in engineering calculations.

Conduction occurs as energy is transported from substance to substance. The *Fourier law of heat conduction* can be expressed as

$$q_x = -kA \frac{dT}{dx} \quad (1.30)$$

where q_x is the heat transfer in x direction, k the *thermal conductivity* (W/mK), A the heat transfer area (m^2), and dT/dx the temperature gradient. The minus sign takes the heat flow positive where the temperature gradient is mathematically negative with respect to x coordinate.

Convection occurs as the energy is transported by the motion of fluid. Although the convective heat transfer appears complicated because of the complex motion of the fluid, the resultant behavior can be expressed in a simple way.

$$q = hA (T_s - T_\infty) \quad (1.31)$$

where h is the *convection heat transfer coefficient* ($\text{W}/\text{m}^2\text{K}$), A the heat transfer area (m^2), T_s the surface temperature, and T_∞ the fluid temperature. This equation is known as *Newton's law of cooling*. Note that the sign convention is such that the heat transfer is positive when the heat flows outward from the surface to the fluid.

Radiation is energy emitted by matter in the form of the electromagnetic waves. Hence, radiation between two objects exchanges their energies. One of the typical radiation problems is a relatively small object in large *surroundings*. In this case, the *radiation exchange* can be expressed as

$$q = A\varepsilon\sigma (T_s^4 - T_{sur}^4) \quad (1.32)$$

where A is the heat transfer area (m^2), ε the *emissivity*, σ the *Stefan-Boltzmann constant* ($\sigma = 5.67 \times 10^{-8} \text{ W}/\text{m}^2 \cdot \text{K}^4$), T_s the absolute temperature (K) of the surface, and T_{sur} the absolute temperature (K) of the surroundings.

1.4.2 Conduction

Consider one-dimensional steady-state conduction in a plane wall where the inner and outer surfaces are in contact with air, as illustrated in Figure 1.6(a). Radiation is neglected. There are three components in the system: inner convection, conduction, and outer convection. Note that the heat transfer in each component must be the same.

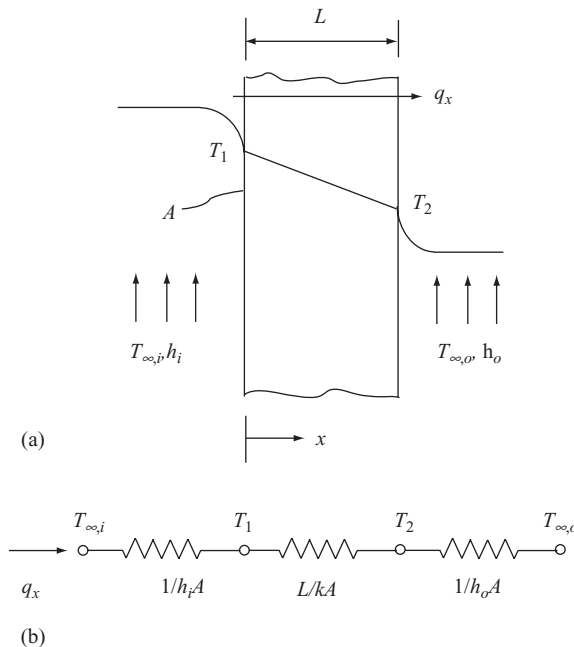


Figure 1.6 Heat transfer through a plane wall: (a) Temperature distribution, (b) The thermal circuit

The convection heat transfer to the plane wall is expressed considering the sign convention discussed previously.

$$q = h_i A (T_{\infty,i} - T_1) = \frac{T_{\infty,i} - T_1}{1/h_i A} = \frac{T_{\infty,i} - T_1}{R_{conv,i}} \quad (1.33)$$

where $R_{conv,i}$ is the *convection thermal resistance* that is defined as $\Delta T/q$. The convection resistance in the inner convection component, $R_{conv,i}$, can be expressed as

$$R_{conv,i} = \frac{1}{h_i A} \quad (1.34)$$

The concept of thermal resistance is similar to that of electrical resistance and is widely used in thermal design. Now consider the conduction in the plane wall. The conduction heat transfer for one-dimensional steady-state conditions is expressed as

$$q = -kA \frac{dT}{dx} = -kA \frac{T_2 - T_1}{L} = \frac{T_1 - T_2}{L/kA} = \frac{T_1 - T_2}{R_{cond}} \quad (1.35)$$

The conduction resistance in the wall is

$$R_{cond} = \frac{L}{kA} \quad (1.36)$$

The convection heat transfer exiting from the wall is

$$q = h_o A (T_2 - T_{\infty,o}) = \frac{T_2 - T_{\infty,o}}{1/h_o A} = \frac{T_2 - T_{\infty,o}}{R_{conv,o}} \quad (1.37)$$

The convection resistance in the outer component is

$$R_{conv,o} = \frac{1}{h_o A} \quad (1.38)$$

Since the system is composed of three components in series, the thermal circuit can be constructed, which is shown in Figure 1.6(b). The *total thermal resistance* will be the sum of the three components.

$$R_{total} = \frac{1}{h_i A} + \frac{L}{kA} + \frac{1}{h_o A} = \frac{\Delta T}{q} \quad (1.39)$$

Now the heat transfer across the wall can be expressed using the total thermal resistance as,

$$q = \frac{T_{\infty,i} - T_{\infty,o}}{\frac{1}{h_i A} + \frac{L}{kA} + \frac{1}{h_o A}} = \frac{T_{\infty,i} - T_{\infty,o}}{R_{total}} \quad (1.40)$$

Note that the calculation of the heat transfer across the wall does not require the inner and outer surface temperatures of the wall. An overall heat transfer coefficient is defined in the following equation as

$$q = UA \Delta T = \frac{\Delta T}{1/UA} \quad (1.41)$$

The overall heat transfer coefficient U is expressed as

$$U = \frac{1}{R_{total}A} \tag{1.42}$$

Sometimes a UA value that is the inverse of the total thermal resistance used in heat exchanger design.

$$UA = \frac{1}{R_{total}} \tag{1.43}$$

Consider a thick tube, where the inner and outer surfaces experience the flows shown in Figure 1.7(a), we find an expression for the heat transfer in a similar way as the plane wall.

$$q = \frac{T_{\infty,i} - T_{\infty,o}}{\frac{1}{h_i (2\pi r_i L)} + \frac{\ln(r_o/r_i)}{2\pi k L} + \frac{1}{h_o (2\pi r_o L)}} = \frac{T_{\infty,i} - T_{\infty,o}}{R_{total}} \tag{1.44}$$

Note that the temperature distribution in the tube is no longer linear as for the one in plane wall because the heat transfer area A increases with increasing the cylindrical coordinate r .

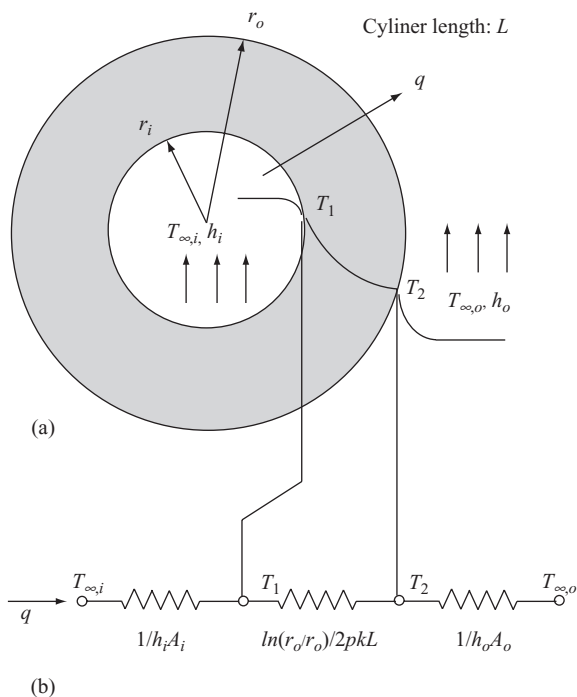


Figure 1.7 Heat transfer through a cylinder: (a) Temperature distribution, (b) Equivalent thermal circuit

1.4.3 Convection

Convection involves not only the heat also the fluid flow. Therefore, energy equations combined with the Navier-Stokes equations should be used to solve the convection problem. *The Navier-Stokes equations* that are composed of the conservation of mass and the conservation of momentum are the fundamental governing equations of fluid flow. These equations were formulated in the early nineteenth century [11, 12], one of the biggest breakthroughs in the field of applied mathematics. However, it is very difficult to solve the equations. A parallel flow over a flat plate (simple but fundamental) was solved by Prandtl [12] in 1904 and Blasius [13] in 1908. Based on those solutions, essential parameters and semiempirical correlations were able to be provided for other cases, which are very useful in thermal design and presented here.

1.4.3.1 Parallel Flow on an Isothermal Plate

Parallel flow on an isothermal flat plate is illustrated in Figure 1.8(a). Assume that uniform *laminar flow* enters from the left. The *boundary layer* physically develops over the plate from the leading edge due to the shear stress (or friction), starting as a laminar boundary layer and at a critical point turning into the turbulent boundary layer as shown. The velocity boundary layer thickness $\delta(x)$ is determined by the velocity, the distance, and the properties of the fluid. A nondimensional number with respect to the distance x along the plate is the *Reynolds number*, Re , defined as

$$Re_x = \frac{\rho U_\infty x}{\mu} = \frac{U_\infty x}{\nu} \quad (1.45)$$

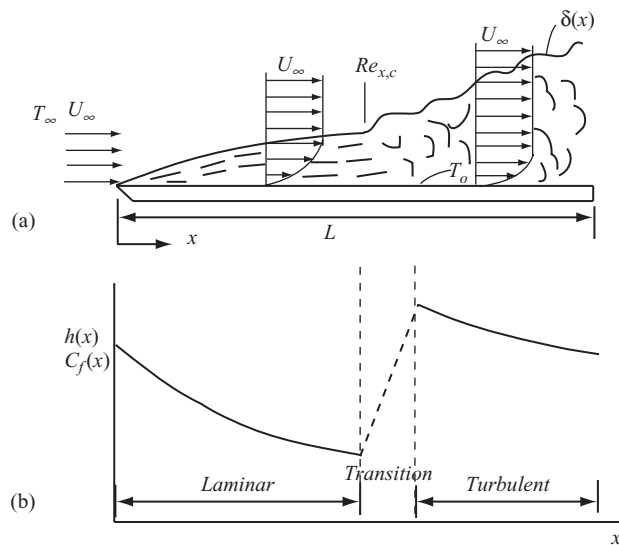


Figure 1.8 Parallel flow on a flat plate: (a) Velocity boundary layer development, (b) Heat transfer coefficient $h(x)$ and friction coefficient $C_f(x)$

In terms of the length L ,

$$Re_L = \frac{\rho U_\infty L}{\mu} = \frac{U_\infty L}{\nu} \quad (1.46)$$

where U_∞ is the entering uniform velocity, ρ the density of the fluid, μ the dynamic viscosity, and L the distance from the leading edge. The meaning of the Reynolds number is the inertia force over the viscous force, which can also be interpreted as a dimensionless velocity. At a critical point, the flow pattern changes from laminar to turbulent flow. *The critical Reynolds number* for a smooth surface has been obtained by measurements, which is

$$Re_{x,c} = 5 \times 10^5 \quad (1.47)$$

As for the velocity boundary layer thickness, the *thermal boundary layer thickness* $\delta_t(x)$ forms in a similar way. The most important dimensionless number (or property) for the thermal boundary layer is the *Prandtl number*, Pr , which is defined as

$$Pr = \frac{\nu}{\alpha} = \frac{\mu c_p}{k} \quad (1.48)$$

where α is the thermal diffusivity, μ the dynamic viscosity, c_p the specific heat at the constant pressure, and k the thermal conductivity of the fluid.

The thermal boundary layer analysis suggests a dimensionless parameter termed *the Nusselt number* Nu_L :

$$Nu_L = \frac{hL}{k} \quad (1.49)$$

The Nusselt number is equal to the dimensionless temperature gradient at the surface or can be interpreted as a dimensionless convection heat transfer coefficient.

There are three important aspects of the convective flow over a flat plate. The first aspect is that the velocity boundary layer thickness is typically very thin (order of millimeters) and the flow beyond the boundary layer behaves as inviscid flow. The velocity adjacent to the surface within the boundary layer causes a shear stress or a friction force on the plate. This is a reason why potential flow (inviscid flow) is still a powerful tool in engineering design. The second aspect is that the transition to *turbulent flow* from *laminar flow* is a very common physical phenomenon (e.g., cigarette's smoke rising becoming turbulent, or turbulence of ship's smoke on the sea—turbulence is due to the infinite distance from the leading edge). If we measure the velocity profile in the turbulent region, we find that the bulk velocity is quite uniform even within the boundary layer as shown, although microscopic eddies prevail all around. The turbulence eventually increases the *friction coefficient* $C_{f,x}$ to some extent, as shown in Figure 1.8(b). This uniformity of the velocity in the boundary layer renders modeling of the turbulent flow feasible. The last aspect is that turbulence causes the convective heat transfer to increase significantly, as shown in Figure 1.8(b). This is an important point for thermal design. For example, turbulent flow could be an option for the enhancement in heat transfer.

Laminar Flow ($Re_L \leq 5 \times 10^5$) The analytical solutions of Prandtl and Blasius provided the following correlations for laminar flow and also the basis for the correlations

for turbulent flow. The local friction coefficient $C_{f,x}$ is

$$C_{f,x} = \frac{\tau_x}{\rho U_\infty^2 / 2} = 0.664 Re_x^{-1/2} \quad (1.50)$$

The average friction coefficient is

$$\bar{C}_f = \frac{\bar{\tau}}{\rho U_\infty^2 / 2} = 1.328 Re_L^{-1/2} \quad (1.51)$$

The local Nusselt number is

$$Nu_x = \frac{h_x x}{k_f} = 0.332 Re_x^{1/2} Pr^{1/3} \quad Pr \geq 0.6 \quad (1.52)$$

The average Nusselt number is

$$\bar{Nu}_L = \frac{\bar{h} L}{k_f} = 0.664 Re_L^{1/2} Pr^{1/3} \quad Pr \geq 0.6 \quad (1.53)$$

Turbulent Flow ($Re_x > 5 \times 10^5$) A turbulent flow is very difficult to solve analytically. Hence, the following correlations mostly rely on experiment. However, the analysis of the laminar flow was very helpful in formulating the correlations for turbulent flow. The *local friction coefficient* is expressed as

$$C_{f,x} = \frac{\tau_x}{\rho U_\infty^2 / 2} = 0.0592 Re_x^{-1/5} \quad 5 \times 10^5 \leq Re_x \leq 10^8 \quad (1.54)$$

The *average friction coefficient* is

$$\bar{C}_f = \frac{\bar{\tau}}{\rho U_\infty^2 / 2} = 0.074 Re_L^{-1/5} \quad 5 \times 10^5 \leq Re_x \leq 10^8 \quad (1.55)$$

The *local Nusselt number* is

$$Nu_x = \frac{h_x L}{k_f} = 0.0296 Re_x^{4/5} Pr^{1/3} \quad 0.6 \leq Pr \leq 60 \text{ and } 5 \times 10^5 \leq Re_x \leq 10^8 \quad (1.56)$$

The *average Nusselt number* for an average heat transfer coefficient for turbulent flow

$$\bar{Nu}_L = \frac{\bar{h} L}{k_f} = 0.037 Re_L^{4/5} Pr^{1/3} \quad 0.6 \leq Pr \leq 60 \text{ and } 5 \times 10^5 \leq Re_x \leq 10^8 \quad (1.57)$$

Mixed Boundary Layer Conditions If the plate has regions where both the laminar and turbulent flows significantly contribute to the heat transfer on the plate, we may use the following correlation:

$$\bar{Nu}_L = \left(0.037 Re_L^{4/5} - 871 \right) Pr^{1/3} \quad 0.6 \leq Pr \leq 60 \text{ and } 5 \times 10^5 \leq Re_x \leq 10^8 \quad (1.58)$$

1.4.3.2 A Cylinder in Cross Flow

For a circular cylinder, the characteristic length is the diameter. In this case, the *Reynolds number* is defined as

$$Re_D = \frac{\rho U_\infty D}{\mu} = \frac{U_\infty D}{\nu} \quad (1.59)$$

A *Nusselt number* is proposed by Churchill and Bernstein [14] for all Re_D and Pr as

$$\overline{Nu}_D = \frac{\overline{h}D}{k} = 0.3 + \frac{0.62 Re_D^{1/2} Pr^{1/3}}{[1 + (0.4/Pr)^{2/3}]^{1/4}} \left[1 + \left(\frac{Re_D}{282,000} \right)^{5/8} \right]^{4/5} \quad (1.60)$$

1.4.3.3 Flow in Ducts

Consider laminar flow in a duct, as shown in Figure 1.9, where fluid enters the duct with a uniform velocity. We know that when the fluid makes contact with the surface, viscous effects become important, and a boundary layer develops with increasing x . This development leads to a boundary layer merger at the centerline. After this merger, the velocity profile no longer changes with increasing x . The flow is said to be *fully developed*. The distance from the entrance to the merger is termed the *hydrodynamic entry length*, $x_{fd,h}$.

The fully developed velocity profile is parabolic for laminar flow in a duct. For turbulent flow, the profile is flatter due to turbulent mixing. When dealing with internal flows, it is important to be cognizant of the extent of the entry region, which depends on whether the flow is laminar or turbulent.

The Reynolds number for flow in a duct is defined as

$$Re_D = \frac{\rho u_m D_h}{\mu} = \frac{u_m D_h}{\nu} \quad (1.61)$$

where u_m is the *mean fluid velocity* over the duct cross section and D_h is the *hydraulic diameter*. The hydraulic diameter is used for noncircular ducts to treat as a circular duct and defined as

$$D_h = \frac{4A_c}{P_{wet}} \quad (1.62)$$

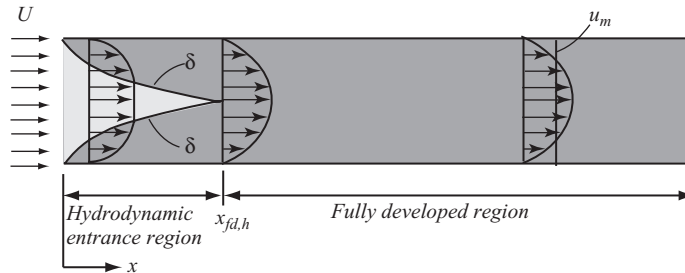


Figure 1.9 Entrance region and fully developed region of laminar flow in a duct

where A_c and P_{wet} are the flow cross-sectional area and the *wetted perimeter*, respectively. The *equivalent diameter* that is used for the heat transfer (*Nusselt number*) calculations is defined as

$$D_e = \frac{4A_c}{P_{heated}} \quad (1.62a)$$

where P_{heated} is the heated perimeter.

The critical Reynolds number corresponding to the onset of turbulence is

$$Re_{D,c} = 2300 \quad (1.63)$$

Although much larger Reynolds numbers ($Re_D = 10,000$) are needed to achieve fully turbulent conditions. The transition to turbulence is likely to begin in the developing boundary layer of the entrance region.

Friction Factor in Fully Developed Flow The engineer is frequently interested in the pressure drop needed to sustain an internal flow because this parameter determines pump or fan power requirements. To determine the pressure drop, it is convenient to work with the *friction factor*, which is a dimensionless parameter.

The *Fanning friction factor* is defined as

$$f_{Fanning} = \frac{\tau_w}{\frac{1}{2}\rho u_m^2} \quad (1.64)$$

where τ_w is the shear stress at wall and u_m is the mean velocity in the duct. The *Darcy friction factor* is defined as

$$f_{Darcy} = \frac{4\tau_w}{\frac{1}{2}\rho u_m^2} \quad (1.65)$$

We adopt herein the Fanning friction factor as is usual in the field of thermal design. Do not confuse it with the Darcy friction factor, often used in other textbooks. For laminar flow, the friction factor is found analytically as

$$f = \frac{16}{Re_D} \quad (1.66)$$

The Fanning friction factor f is presented graphically in Figure 1.10, where the friction factor for laminar flow and turbulent flow are plotted with the various roughness of the surface of the duct. The transition at $Re_D = 2,300$ from the laminar region to the turbulent region is apparent in the figure.

For smooth circular ducts in turbulent flow, the friction factor suggested by Filonenko [15] for $10^4 < Re_D < 10^7$ is given by

$$f = (1.58 \ln(Re_D) - 3.28)^{-2} \quad (1.67)$$

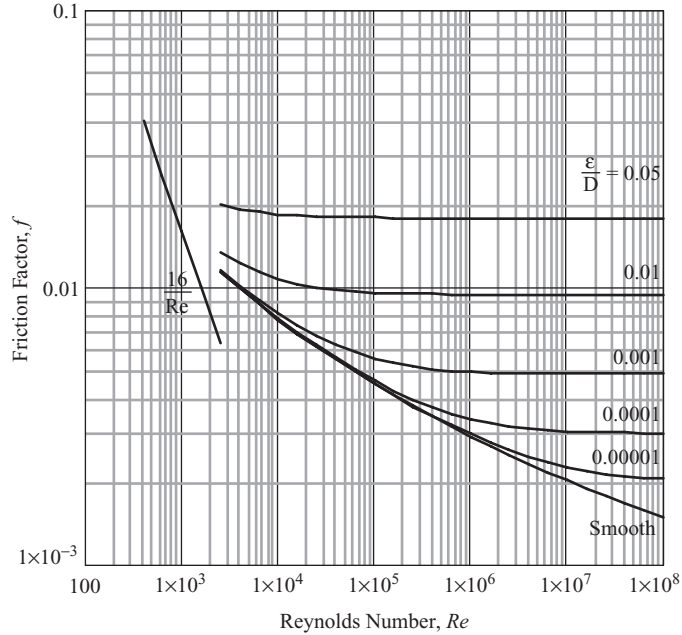


Figure 1.10 Fanning friction factor as a function of Reynolds number for pipe flow

Pressure Drop The friction causes the pressure drop that can be easily derived from taking the force balance on a differential element in pipe flow. The pressure drop is given by

$$\Delta P = \frac{4fL}{D_h} \frac{\rho u_m^2}{2} = \frac{2fL}{D_h} \frac{G^2}{\rho} \quad (1.68)$$

where G is the mass velocity,

$$G = \rho u_m \quad (1.69)$$

Pump or Fan Power The power of a fan or pump may be calculated by

$$\dot{W}_{actual} = \frac{dW}{dt} = \frac{\dot{m}}{\eta_p \rho} \Delta P \quad (1.70)$$

where η_p is the pump efficiency and \dot{m} the mass flow rate.

Laminar Flow ($Re_D < 2300$) For laminar flow, the hydrodynamic entry length is approximately calculated as

$$\left(\frac{x_{fd,h}}{D_h} \right)_{lam} \approx 0.05 Re_D \quad (1.71)$$

For laminar flow, the thermal entry length may be expressed as

$$\left(\frac{x_{fd,t}}{D_h} \right)_{lam} \approx 0.05 Re_D Pr \quad (1.72)$$

A general relation for the combined entry length for the hydrodynamic and thermal entry and fully developed laminar flow is given by Sieder and Tate [16]. The average Nusselt number is

$$\overline{Nu}_D = \frac{\overline{h}D}{k} = 1.86 \left(\frac{Re_D Pr}{L/D} \right)^{\frac{1}{3}} \left(\frac{\mu}{\mu_s} \right)^{0.14} \quad 0.6 < Pr < 5 \quad (1.73)$$

where all the properties are evaluated at mean temperature except μ_s , which is the absolute viscosity evaluated at the wall temperature.

The Nusselt number Nu and the friction factor f are given in Table 1.1 for fully developed laminar flow in ducts of various cross-sections.

Turbulent Flow ($Re_D > 2,300$) Since turbulent flow is ubiquitous in fluid flow, greater emphasis is placed on determining empirical correlations. For turbulent fully developed flow, the Dittus-Boelter equation [23] based on the Colburn equation has been widely used. The Nusselt number is given by

$$Nu_D = \frac{hD}{k} = 0.023 Re_D^{4/5} Pr^n \quad 0.6 \leq Pr \leq 160 \text{ and } Re_D \geq 10,000 \quad (1.74)$$

where $n = 0.4$ for $T_s > T_{mean}$ and $n = 0.3$ for $T_s < T_{mean}$. This equation has been confirmed experimentally for a range of conditions.










Although Equation (1.74) is easily applied and is mostly satisfactory, errors may be as large as 25 percent. Such errors may be reduced to less than 10 percent through the use of a more recent correlation. Gnielinski [17] recommended the following correlation valid over a large Reynolds number range, including the transition region. The *Nusselt number* for turbulent is

$$Nu_D = \frac{hD}{k} = \frac{(f/2)(Re_D - 1000)Pr}{1 + 12.7(f/2)^{1/2}(Pr^{2/3} - 1)} \quad (1.75)$$

$$3000 < Re_D < 5 \times 10^6 \text{ and } 0.5 \leq Pr < 2,000$$

where the friction factor f is obtain from Equation (1.67).

Table 1.1 Nusselt Numbers and Friction Factors for Fully Developed Laminar Flow in Tubes of Differing Cross-sections

Cross-section	Aspect ratio	$Nu = h \cdot D/k$		Friction factor $f \cdot Re_D$
		Uniform Q''	Uniform T_o	
	—	4.36	3.66	16
	—	2.47	3.11	13
	1.0	3.61	2.98	14
	1.43	3.73	3.08	15
	2.0	4.12	3.39	16
	3.0	4.79	3.96	17
	4.0	5.33	4.44	18
	8.0	6.49	5.6	20
	∞	8.23	7.54	24

1.4.3.4 Free Convection

Free convection, also referred to as *natural convection*, is an important mechanism responsible for heat transfer in our ordinary life. Candlelight would not be possible without free convection. The hot air adjacent to the flame rises due to buoyancy (the warm air is lighter than the cold air) and the cold air replaces the hot air (this supplies oxygen) so that the candle continues burning.

There was actually an experiment for candlelight in space. The result showed that the flame was extinguished after a short period of time. For another example, you would wait a long time in order to have a boiled egg if there were no free convection. Heat transfer from the bodies of animals and human beings are free convection. Today, the cooling of house appliances such as refrigerators and TV (electronics) is based on free convection. It is interesting to note that the driving force of free convection is buoyancy, which results from gravity. We want to here consider a simple, but important, geometry, a vertical plate.

Isothermal Vertical Plate Consider a heated vertical plate at T_s in quiescent air at T_∞ where $T_s > T_\infty$, as shown in Figure 1.11. As for the flow over a flat plate, this problem involves the Navier-Stokes equation and the energy equation with a gravity effect. These equations were solved in the 1930s using the *similarity variable method* and turning them into two ordinary equations that are solvable. The schematic profiles for the temperature and velocity from the solution are illustrated in the figure. Today every heat transfer book includes these results, which are in a good agreement with measurements. More important is that the analysis provided very important parameters. These parameters are the *Grashof number* and *Prandtl number*. The product of the

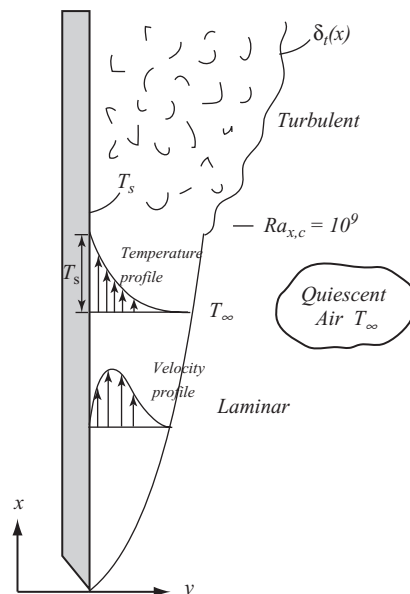


Figure 1.11 Free convection boundary layer transition on a vertical plate

Grashof and Prandtl numbers is the *Rayleigh number*, which is defined as

$$Ra_L = Gr \cdot Pr = \frac{g\beta(|T_s - T_\infty|)L^3}{\nu^2} \cdot \frac{\nu}{\alpha} = \frac{g\beta(|T_s - T_\infty|)L^3}{\nu\alpha} \quad (1.76)$$

where g is the gravity, β the *expansion coefficient*, ν the *kinematic viscosity*, and α the *thermal diffusivity*. The number should be positive always.

The results from the solution for the governing equations can be further simplified. Then, the average Nusselt number for an isothermal vertical plate is expressed by two separate equations as

$$\overline{Nu} = \frac{\overline{h}L}{k} = 0.59Ra_L^{\frac{1}{4}} \quad \text{for } Ra_L \leq 10^9 \quad (1.77a)$$

$$\overline{Nu} = \frac{\overline{h}L}{k} = 0.10Ra_L^{\frac{1}{3}} \quad \text{for } Ra_L > 10^9 \quad (1.77b)$$

In the special case of air, the following correlation was suggested by LeFevre [18]:

$$\overline{Nu} = \frac{\overline{h}L}{k} = 0.517Ra_L^{\frac{1}{4}} \quad \text{for } Pr = 0.72 \text{ (air)} \quad (1.77c)$$

A correlation that may be applied over the entire range of Ra_L has been recommended by Churchill and Chu [19]. It is of the form

$$\overline{Nu} = \frac{\overline{h}L}{k} = \left\{ 0.825 + \frac{0.387Ra_L^{\frac{1}{6}}}{[1 + (0.492/Pr)^{9/16}]^{4/9}} \right\}^2 \quad (1.78)$$

Isothermal Parallel Vertical Plates Vertical fins are a very common geometry for heat sinks. We want to consider two isothermal vertical plates—a small spacing channel and a large spacing channel. When the spacing is close, the flow will be fully developed with a parabolic profile, as shown in Figure 1.12(a). On the one hand, if the spacing is too close, there will be no flow because of the friction on each plate. On the other hand, when the spacing is large, each velocity boundary layer will be isolated and behave as if the fluid flows over a single vertical plate, as shown in Figure 1.12(b).

In the design of a heat sink (array of fins), an increase in the heat transfer area, which is equivalent to increasing the number of fins within a given base area, is required in order to reduce the thermal resistance (or decrease the base temperature). The spacing z decreases with an increased number of fins, leading to a decrease in the convection coefficient due to the closeness. Therefore, an optimum spacing exists. Here we want to provide a correlation for the average Nusselt number.

Elenbaas [20] provided the experimental data, which are shown in Figure 1.13, where the Elenbaas number based on the Rayleigh number was used. The Rayleigh number is based on plate spacing:

$$Ra_z = \frac{g\beta(|T_s - T_\infty|)z^3}{\nu\alpha} \quad (1.79)$$

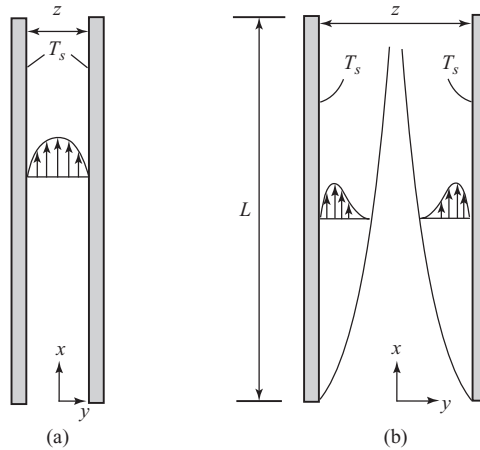


Figure 1.12 Natural convection for fully developed flow in (a) small spacing channel and (b) large spacing channel

where z is the fin spacing. Caution is given for the spacing z to be used in place of length L (see Equation (1.76)). Then, the Elenbaas number El is defined by

$$El = Gr \cdot Pr \frac{z}{L} = Ra_z \frac{z}{L} = \frac{g\beta(|T_s - T_\infty|)z^4}{\nu\alpha L} \quad (1.80)$$

Using the composite relation method, the Elenbaas data were curve fitted. The average Nusselt number is expressed as [21]

$$\overline{Nu}_z = \frac{\overline{h}_z z}{k} = \left[\frac{576}{El^2} + \frac{2.873}{El^{1/2}} \right]^{-1/2} \quad (1.81)$$

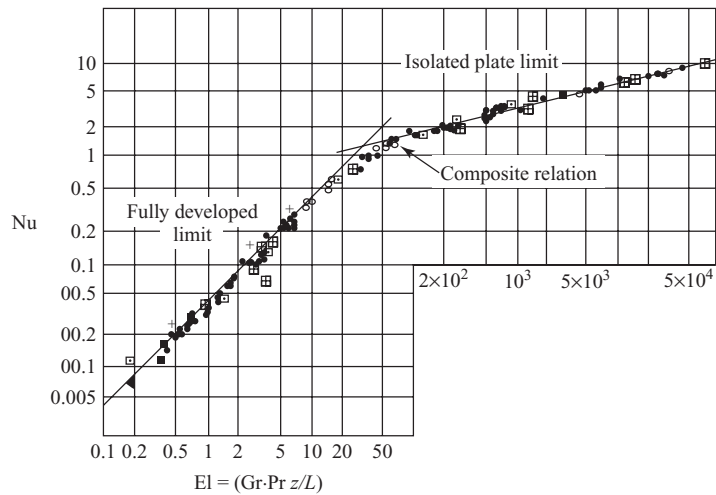


Figure 1.13 Nusselt number variation for vertical isothermal plates (data points from Elenbaas, 1942 [20])

Horizontal Cylinder For a long horizontal isothermal cylinder, Churchill and Chu [22] suggested a correlation for the average Nusselt number. Note that the Rayleigh number Ra_D uses the cylinder diameter D .

$$Ra_D = Gr \cdot Pr = \frac{g\beta(|T_s - T_\infty|)D^3}{\nu^2} \cdot \frac{\nu}{\alpha} = \frac{g\beta(|T_s - T_\infty|)D^3}{\nu\alpha} \quad (1.82)$$

The average Nusselt number for the free convection of the horizontal cylinder is

$$\overline{Nu}_D = \frac{\overline{h}D}{k} = \left\{ 0.60 + \frac{0.387Ra_D^{1/6}}{[1 + (0.559/Pr)^{9/16}]^{8/27}} \right\}^2 \quad (1.83)$$

1.4.4 Radiation

1.4.4.1 Thermal Radiation

Radiation is electromagnetic waves (or photons), propagating through a transparent medium (air) or even effectively in a vacuum as one of the heat transfer mechanisms. Radiation is a spectrum with a wide range of the wavelengths, from microwaves to gamma rays. Thermal radiation encompasses a range from infrared to ultraviolet, which includes visible light. A rainbow assures us that the light is indeed a spectrum. The surface of any matter emits electromagnetic radiation if the temperature of the surface is greater than absolute zero. It also absorbs radiation from the surroundings, which is called *irradiation*. The *emissivity* and *absorptivity*, lying between 0 and 1, of real bodies vary, depending on the finishes of the surfaces and the nature of the irradiation. This feature provides engineers with potential for improvement in the control of heat transfer. A perfect emitter, perfect absorber, and also perfect diffuser is called a *blackbody*. Two properties of radiation that have importance here are its *spectrum* and *directionality*.

The spectral emissive powers of a blackbody and a real surface are illustrated in Figure 1.14, where the emissive power of the real surface is always less than that of the blackbody.

The second property of thermal radiation relates to its directionality, as shown in Figure 1.15. A *blackbody* has a *diffuse* property.

Blackbody A *blackbody* is a perfect emitter and absorber. A blackbody emits radiation energy uniformly in all directions (i.e., a *diffusive emitter*). *Plank's law* provides the spectral distribution of blackbody emission:

$$E_{\lambda,b}(\lambda, T) = \frac{C_1}{\lambda^5 [\exp(C_2/\lambda T) - 1]} \quad (1.84)$$

where $C_1 = 3.472 \times 10^8 \text{ W} \cdot \mu\text{m}^4/\text{m}^2$ and $C_2 = 1.439 \times 10^4 \mu\text{m} \cdot \text{K}$. This is a function of both wavelength and temperature, as shown in Figure 1.16, where the spectral emissive power distribution is dependent on the temperature and wavelength.

If we integrate the spectral distribution, Equation (1.84), with respect to wavelength λ over the entire range from $\lambda = 0$ to $\lambda = \infty$, we have the total emissive power of the blackbody, which is known as the *Stefan-Boltzmann law*. The *total emissive power* is

$$E_b = \sigma T^4 \quad (1.85)$$

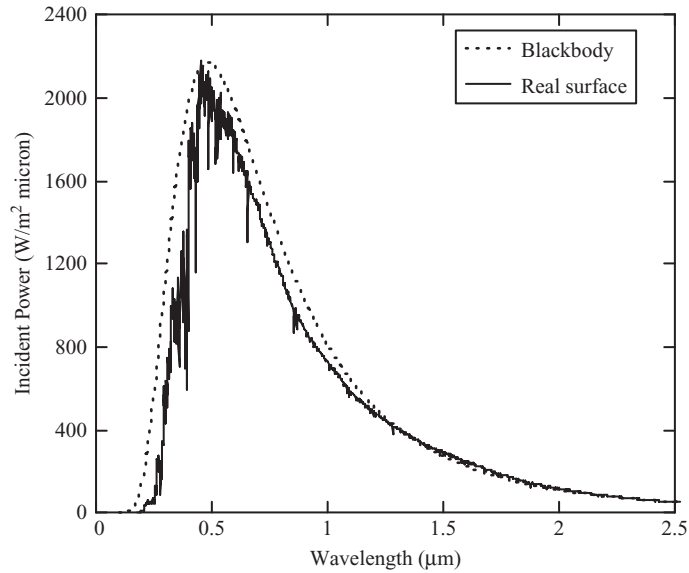


Figure 1.14 Spectral distributions of a blackbody and a real surface

where E_b is the total emissive power of a blackbody and T is the surface temperature of the body and $\sigma = 5.67 \times 10^{-8} \text{ W/m}^2 \cdot \text{K}^4$, which is termed the *Stefan-Boltzmann constant*.

Therefore, the emissive power of a real surface is

$$E = \varepsilon \sigma T^4 \quad (1.86)$$

where ε is the *emissivity*.

Irradiation G Irradiation G is an incident radiation, which may originate from other surfaces or from the surroundings, being independent of the finishes of the intercepting surface. Irradiation will have spectral and directional properties. Irradiation could be

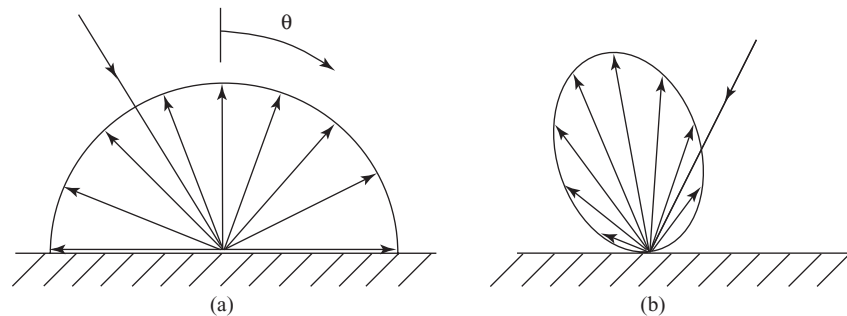


Figure 1.15 Comparison of blackbody and real surface (a) diffuse, and (b) directional

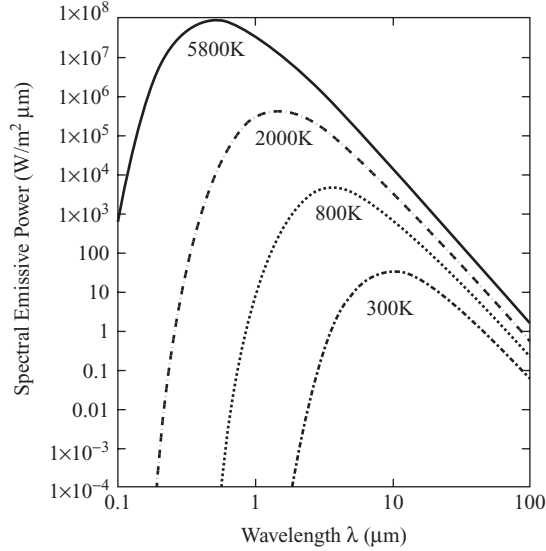


Figure 1.16 Spectral blackbody emissive power

partially absorbed, reflected, or transmitted, as shown in Figure 1.17.

$$\rho + \alpha + \gamma = 1 \tag{1.87}$$

where ρ is the *reflectivity*, α is the *absorptivity*, and γ is the *transmissivity*.

For instance, if the surface is opaque, the transmissibility γ is zero.

$$\rho + \alpha = 1 \tag{1.88}$$

Radiosity J Radiosity J is all the radiant energy leaving a surface, consisting of the direct emission ϵE_b from the surface and the reflected portion ρG of the irradiation, as shown in Figure 1.17. The radiosity is

$$J = \epsilon E_b + \rho G \tag{1.89}$$

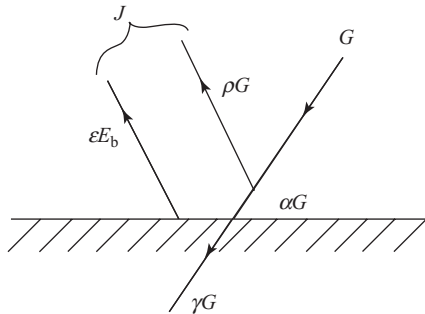


Figure 1.17 Surface radiosity J includes emission ϵE_b and reflection ρG ; irradiation G includes absorption αG , reflection ρG , and transmission γG

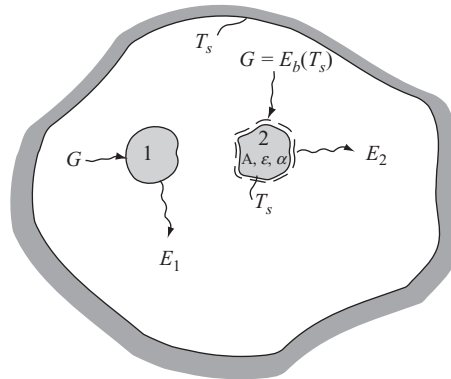


Figure 1.18 Radiation exchange in an isothermal enclosure

Kirchhoff's Law Consider a large, isothermal enclosure at surface temperature T_s , within which several small bodies are confined, as shown in Figure 1.18. Under steady-state conditions, thermal equilibrium must exist between the bodies and the enclosure. Regardless of the orientation and the surface properties of the enclosure, the irradiation experienced by any body in the enclosure must be diffuse and equal to emission from a blackbody at T_s .

The irradiation in the *enclosure* behaves like a blackbody.

$$G = E_b(T_s) \quad (1.90)$$

The absorbed irradiation is

$$G_{abs} = \alpha G = \alpha \dot{E}_b(T_s) \quad (1.91)$$

At thermal equilibrium, the energy absorbed by the body must be equal to the energy emitted. Otherwise, there would be an energy flow into or out of the body that would raise or lower its temperature. For a body denoted by 2, the energy balance gives

$$A_2 \alpha_2 G - A_2 E_2 = 0 \quad (1.92)$$

Or equivalently,

$$\alpha_2 E_b(T_s) - \varepsilon_2 E_b(T_s) = 0 \quad (1.93)$$

Eventually,

$$\alpha_2 = \varepsilon_2 \quad (1.94)$$

The same thing happens for the other bodies. Therefore, in an enclosure, we have

$$\alpha = \varepsilon \quad (1.95)$$

The total emissivity of any surface is equal to its total absorptivity, which is known as the *Kirchhoff's law*. Since we know that radiation inherently has spectral and directional properties, $\alpha_{\lambda, \theta} = \varepsilon_{\lambda, \theta}$, we conclude that radiation in an enclosure is independent of the spectral and directional distributions of the emitted and incident radiation. Note that this relation is derived under the condition that the surface temperature of the body

is equal to the temperature of the source of the irradiation. However, since ε and α vary weakly with temperature, this relation may be assumed and greatly simplifies the radiation calculation.

Gray Surface A *gray surface* is defined as one for which α_λ and ε_λ are independent of wavelength λ over the spectral range of the irradiation and the surface emission.

Diffuse-Gray Surface A common assumption in enclosure calculations is that surfaces are *diffuse-gray*. The diffuse-gray surface emits and absorbs a fraction of radiation for all directions and all wavelengths. For a diffuse-gray surface, total emissivity and absorptivity are equal. The total absorptivity is independent of the nature of the incident radiation.

Radiation Exchange for a Single Surface in an Enclosure Consider a *diffuse-gray surface* at T_s in an enclosure (surroundings) at T_{sur} . Equation (1.95) can be applied with the assumption of the diffuse-gray surface in the enclosure. The net radiation exchange of the surface is obtained as

$$q = A\varepsilon\sigma (T_s^4 - T_{sur}^4) \quad (1.96)$$

1.4.4.2 View Factor

The *view factor* F_{ij} is defined as the fraction of the radiation leaving surface i that is intercepted by surface j , as shown in Figure 1.19. Some typical view factors are illustrated in Table 1.2. Consider radiative heat transfer between two or more surfaces, which is often the primary quantity of interest in fin design. Two important relations are suggested:

Reciprocity relation:

$$A_i F_{ij} = A_j F_{ji} \quad (1.97)$$

Summation rule:

$$\sum_{j=1}^N F_{ij} = 1 \quad (1.98)$$

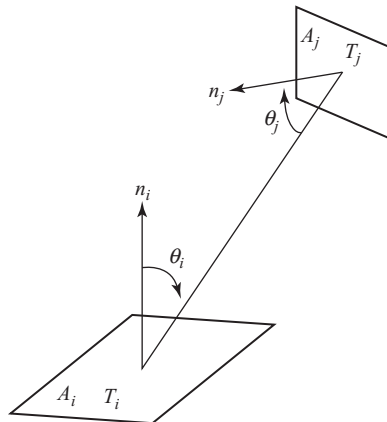


Figure 1.19 View factor associated with radiation exchange between two finite surfaces

Table 1.2 View Factors for Two- and Three-dimensional Geometries

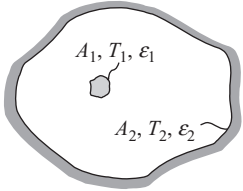
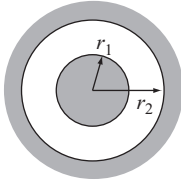
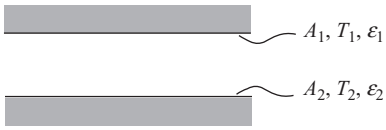
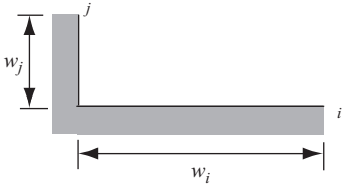
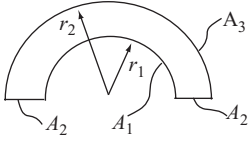
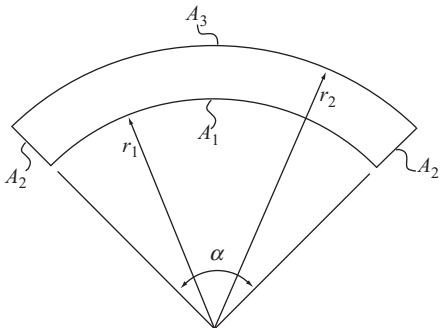
Configuration	View factor
<p>1. Small Object in a Large Cavity</p> 	$\frac{A_1}{A_2} = 0 \quad F_{12} = 1 \quad (1.99)$
<p>2. Concentric Cylinder (infinite length)</p> 	$\frac{A_1}{A_2} = \frac{r_1}{r_2} \quad F_{12} = 1$ $F_{21} = \frac{A_1}{A_2} F_{12} \quad (1.100)$ $F_{22} = 1 - \frac{A_1}{A_2} F_{12}$
<p>3. Large (infinite) Parallel Plate</p> 	$A_1 = A_2 = A \quad F_{12} = 1 \quad (1.101)$
<p>4. Perpendicular plates with a common edge</p> 	$F_{ij} = \frac{1 + w_j/w_i - \left[1 + (w_j/w_i)^2\right]^{1/2}}{2} \quad (1.102)$
<p>5. Hemispherical concentric cylinder</p> 	$F_{13} = \frac{1}{2} + \frac{1}{\pi} \left(\frac{r_2}{r_1}\right) \left[1 - \left(\frac{r_1}{r_2}\right)^2\right]^{1/2} + \frac{1}{\pi} \sin^{-1} \left(\frac{r_1}{r_2}\right) - \frac{1}{\pi} \frac{r_2 - r_1}{r_1} \quad (1.103)$

Table 1.2 (continued)

Configuration	View factor
<p>6. Concentric cylinder (infinite length) with variable angle α</p>  <p>$0 \leq \alpha \leq \pi$</p>	<p>If $\alpha \geq \cos^{-1}\left(\frac{r_1}{r_2}\right)$ (1.104)</p> $F_{13} = 1 - \frac{\pi}{2\alpha} + \frac{r_2}{\alpha r_1} \left[1 - \left(\frac{r_1}{r_2}\right)^2 \right]^{1/2} + \frac{1}{\alpha} \cdot \sin^{-1}\left(\frac{r_1}{r_2}\right) - \frac{r_2 - r_1}{\alpha r_1}$ $F_{22} = \frac{2\sqrt{r_2^2 - r_1^2} + 2r_1 \left[\alpha - \frac{\pi}{2} + \sin^{-1}\left(\frac{r_1}{r_2}\right) \right] - \alpha (r_2 + r_1)}{4 (r_2 - r_1)}$ <p>Otherwise</p> $F_{13} = \frac{\sqrt{r_2^2 + r_1^2 - 2r_2r_1\cos(\alpha)} - (r_2 - r_1)}{\alpha r_1}$ $F_{22} = \frac{2\sqrt{r_2^2 + r_1^2 - 2r_2r_1\cos(\alpha)} - \alpha (r_2 + r_1)}{4 (r_2 - r_1)}$

1.4.4.3 Radiation Exchange between Diffuse-Gray Surfaces

The net rate of heat transfer at a surface is obtained by applying heat balance on the control volume at the surface (see Figure 1.20).

The *diffuse-gray surface* in an enclosure has

$$\epsilon_i = \alpha_i \tag{1.105}$$

The heat balance at the surface gives

$$q_i = A_i(\epsilon_i E_{bi} - \alpha_i G_i) \tag{1.106}$$

The net rate of heat transfer is also equal to the difference between the surface radiosity and the irradiation.

$$q_i = A_i(J_i - G_i) \tag{1.107}$$

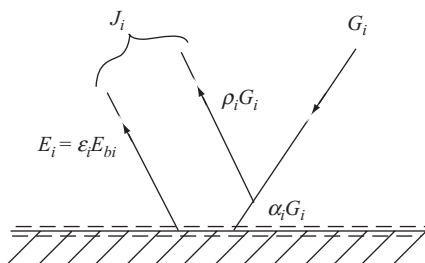


Figure 1.20 Radiation exchange on an opaque, diffuse-gray surface

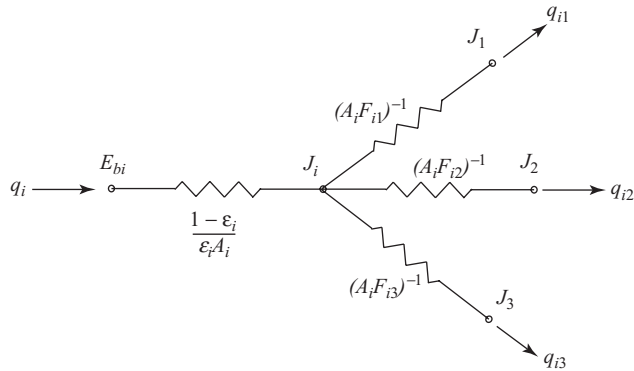


Figure 1.21 Radiation network between surface i and the remaining surfaces of the enclosure

Combining these three equations and eliminating the irradiation G_i gives

$$q_i = \frac{E_{bi} - J_i}{(1 - \epsilon_i)/\epsilon_i A_i} \quad (1.108)$$

The *net radiation exchange* between the radiosities in the enclosure is

$$q_{ij} = \frac{J_i - J_j}{(A_i F_{ij})^{-1}} \quad (1.109)$$

The net rate of heat transfer at surface i is connected to the number of radiosities in the enclosure and forms a radiation network (Figure 1.21).

$$q_i = \sum_{j=1}^N \frac{J_i - J_j}{(A_i F_{ij})^{-1}} \quad (1.110)$$

Combining Equations (1.108) and (1.110), we obtain

$$\frac{E_{bi} - J_i}{(1 - \epsilon_i)/\epsilon_i A_i} = \sum_{j=1}^N \frac{J_i - J_j}{(A_i F_{ij})^{-1}} \quad (1.111)$$

REFERENCES

1. W.F. Stoecker, *Design of Thermal Systems* (3rd ed.). New York: McGraw-Hill, 1989.
2. Y. Jaluria, *Design and Optimization of Thermal Systems*. New York: McGraw-Hill, 1998.
3. A. Bejan, G. Tsatsaronis, and M. Moran, *Thermal Design and Optimization*. New York: John Wiley and Sons, 1996.
4. B.K. Hodge and R.P. Taylor, *Analysis and Design of Energy Systems* (3rd ed.). Englewood Cliffs, NJ: Prentice Hall, 1999.
5. L.C. Burmeister, *Elements of Thermal-Fluid System Design*. Englewood Cliffs, NJ: Prentice Hall, 1998.

6. W.S. Janna, *Design of Fluid Thermal Systems* (2nd ed.). Boston: PWS Publishing Company, 1998.
7. N.V. Suryanarayana and O. Arici, *Design of Simulation of Thermal Systems*. New York: McGraw-Hill, 2003.
8. A. Ertas and J.C. Jones, *The Engineering Design Process* (2nd ed.). New York: John Wiley and Sons, 1993.
9. C.L. Dym and P.L. Little, *Engineering Design: A Projected-Based Introduction*. New York: John Wiley and Sons, 2000.
10. C.L.M.H. Navier, Memoire sur les lois du mouvement des fluids, *Mem. Acad. R. Sci. Paris*, 6 (1823): 389–416.
11. G.G. Stokes, On the Theories of Internal Friction of Fluids in Motion, *Trans. Cambridge Phil. Soc.*, 8 (1845): pp. 145–239.
12. L. Prandtl, Über Flussigkeitsbewegung bei she kleiner Reibung, *Proc. 3rd Int. Math. Congr.* (Heidelberg 1904); NACA TM 452, 1928.
13. H. Blasius, Grenzschichten in Flüssigkeiten mit kleiner Reibung, *Z. Math. Phys.*, 56 (1908): 1–37; also in English as The Boundary Layers in Fluids with Little Friction, NACA TM 1256.
14. S.W. Churchill and M. Bernstein, *J. Heat Transfer.*, 99 (1977): 300.
15. G.K. Filonenko, Hydraulic Resistance in Pipes (in Russian), *Teplonergetika*, Vol. 1, pp. 40–44, 1954.
16. E.N. Sieder and G.E. Tite, Heat Transfer and Pressure Drop of Liquids in Tubes, *Ind. Eng. Chem.*, 28 (1936): 1429.
17. V. Gnielinski, New Equation for Heat and Mass Transfer in Turbulent Pipe and Channel Flow. *Int. Chem., Eng.*, 16 (1976): 359–368.
18. E.J. LeFevre, Laminar Free Convection from a Vertical Plane Surface, *Proc. 9th int. Congr. Applied Mech.* Brussels, 4 (1956): 168–174.
19. S.W. Churchill and H.H.S. Chu, Correlating Equations for Laminar and Turbulent Free Convection from a Vertical Plate, *Int. J. Heat Mass Transfer*, 18 (1975): 1323–1329.
20. W. Elenbaas, Heat Distribution of Parallel Plates by Free Convection, *Physica*, 9 (1) (1942): 665–671.
21. A.D. Klaus and A. Bar-Cohen, *Design and Analysis of Heat Sinks*. New York: John Wiley and Sons, 1995.
22. S.W. Churchill and H.H.S. Chu, *Int. J. Heat Mass Transfer*, 18 (1975): 1049.
23. R.H. Winterton, *Int. J. Heat Mass Transfer*, 41 (1998): 809.